Journal of Geosciences and Geomatics, 2019, Vol. 7, No. 4, 201-211
Available online at http://pubs.sciepub.com/jgg/7/4/5
Published by Science and Education Publishing
DOI:10.12691/jgg-7-4-5

Evaluation of Five Tropospheric Delay Models on Global Navigation Satellite System Measurements in Southern Nigeria

Dodo J. D.[1,*], Ekeanyanwu U. O.[2], Ono M. N.[2]

[1]Centre for Geodesy and Geodynamics, National Space Research and Development Agency, Toro, Nigeria
[2]Department of Surveying and Geoinformatics, Nnamdi Azikiwe University, Awka
*Corresponding author: jd.dodo@gmail.com

Received July 29, 2019; Revised September 02, 2019; Accepted September 15, 2019

Abstract Throughout Nigeria, the structure and facilities needed for the operation of a Global Navigation Satellite System (GNSS) based Continuously Operating Reference Stations (CORS) has been set up at different locations in the country generally known as NIGerian Reference GNSS NETwork (NIGNET) for surveying and mapping. Different researchers have conducted investigations into the effect of the troposphere over the NIGNET. This study aims at comparing analytically the effect of five different a priori tropospheric models on GNSS signals in Southern Nigeria with a view to obtaining the best-fit model. The objectives include evaluation of the global tropospheric models in the baseline and position domain; and determining the best model for southern Nigeria. Observational data used were obtained from Office of Surveyor General of Nigerian Mapping Agency (OSGoF). GPS data were obtained from October 2010, to April 2011. Six processing strategies were employed these include; application of no model, application of five global tropospheric delay models (Black, Davis et al, Hopfield, Neil and Saastamoinen) models using Trimble Total Control software version 2.73. Each of the strategies went through free and constrained adjustments and the results were compared. The five models investigated show no significance difference in their performance; better improvements in the position domain were achieved by the application of the Niell model compared to the rest of the models. The Niell model produced a better mitigation of the tropospheric delay, with an average percentage improvement of 67.1%; while Davis et al, the modified Hopfield and Saastaminen models have 70%, 71.1% and 71.7% percentage improvement respectively. The result also indicates that, the Neill model gave the best result and a better improvement in the entire network with the lowest mean average zenith tropospheric delay (ZTD) of 2.535m and least average RMSE of 0.67m. The specific objective of this study is to determine the best tropospheric delay for the study area and to recommend to practicing Surveyor on the model to be used. The research shows that, the Neil model gives the best result when compared with other model. Hence, it is recommended when processing GNSS observations for tropospheric delay to obtain a more accurate result.

Keywords: *tropospheric delay model, saastamoinen, Niell, hopfield, davis et al, black model*

Cite This Article: Dodo J. D., Ekeanyanwu U. O., and Ono M. N., "Evaluation of Five Tropospheric Delay Models on Global Navigation Satellite System Measurements in Southern Nigeria." *Journal of Geosciences and Geomatics*, vol. 7, no. 4 (2019): 201-211. doi: 10.12691/jgg-7-4-5.

1. Introduction

The Earth's atmosphere has a series of layers, each with its own specific traits. Moving upward from ground level, these layers are named the troposphere, stratosphere, mesosphere, thermosphere and exosphere. The troposphere is the lowest layer of the Earth's atmosphere. It is the layer of the atmosphere, which we live in, where the weather happens and most clouds are found. The troposphere starts at Earth's surface and goes up to a height of 7 to 20km (4 to 12 miles) above sea level. Most of the mass (about 75 – 80%) of the atmosphere is in the troposphere. The height of the troposphere depends on the latitude, season, and whether it is day or night [1].

Water vapour contained in the atmosphere can also affect the GPS signal. GPS signal is being affected by the troposphere both horizontally and vertically. The effect can result in position degradation can be reduced by using atmospheric models. Several standard tropospheric models are generally used to correct for the tropospheric delay. In this work, five tropospheric delay models are considered [2,3,4,5].

The delay caused by the troposphere can be separated into two main components: the dry delay and the wet delay. The dry component contributes about 90% of the total delay to the tropospheric delay, while the wet component contributes the remaining 10% of the total tropospheric delay. The dry component is determined with high accuracy by many tropospheric delay models derived from surface measurements [2,6,7]. The wet component

depends on water vapour content, which is highly variable with space and time and is difficult to model [8,9,10]. Although the wet component of the delay constitutes 10% of the total effect, it still causes the limiting uncertainty in determining a very accurate remedy for the total delay [6,11].

The assessment of the five tropospheric delay models is to determine the best-fit model for Southern Nigeria. Although [12] determined the best-fit model for Nigeria, only three models (Saastamoinen, Modified Hopfield, and Neil) were evaluated. This research added two models (Davis et al and Black models) in addition to the models used in [12].

2. Tropospheric Delay

The effect of the troposphere on the GNSS signal appears as an extra delay in the measurement of the signal travelling from the satellite to receiver. This delay is caused by the changing humidity, temperature and atmospheric pressure in the troposphere as well as the transmitter and receiver antennas location. This allows Differential GNSS and RTK systems to compensate for tropospheric delay. GNSS receivers can also use tropospheric models to estimate the amount of error caused by tropospheric delay. The sources of errors are satellite clock, receiver clock, satellite orbit, multipath effect, and atmospheric effects (ionosphere and troposphere). Unlike the ionospheric delay, the tropospheric delay is not frequency-dependent. It cannot therefore be eliminated through linear combinations of L1 and L2 observations. Signals from satellites at low elevation angles have longer propagation period through the troposphere than those of higher elevation angles, the effect of which results in minimized tropospheric delay at the user's zenith (about 2 - 2.5m) and maximum delay at the horizon (about 20 – 28m) [13]. It is thus obvious that the tropospheric delay should be a spatio-temporal variable with its effects differing based on temperature, humidity and pressure.

Due to the highly variable tropospheric water vapour content, it is difficult to achieve desired accuracy in this region [14]. The tropospheric delay in equation (1) is directly proportional to the refractive index, which is expressed as a function of atmospheric temperature and pressure. It is therefore expressed as [13]:

$$D^{trop} = \int (n-1)\,ds \tag{1}$$

where D^{Trop} is the tropospheric delay, n is the refractive index and ds is the path length.

The refractivity can be divided into dry and water vapour due to the troposphere containing dry and water vapour content, hence;

$$N = N_d + N_w \tag{2}$$

where, N_d: refractivity of dry air N_w: refractivity of water vapour. Expressing in terms of refractivity N; from equation (1); we obtain;

$$N^{trop} = 10^{-6}(n-1) \tag{3}$$

where; N^{trop} : tropospheric refractivity, hence;

$$D^{trop} = 10^{-6}\int N^{trop}\,ds. \tag{4}$$

The tropospheric delay can be separated into the dry and wet components as shown in Figure 1.

$$N^{trop} = N_d^{trop} + N_w^{trop} \tag{5}$$

where; (N_d^{trop}) is the dry tropospheric refractivity and (N_w^{trop}) wet tropospheric refractivity resulting from water vapour.

The dry and wet components as shown in Figure1are as a result of dry gases (primary nitrogen and oxygen) and water vapour respectively in the tropospheric region of the atmosphere. About 90% of the tropospheric delay is caused by the dry component, while the remaining 10% is from the wet component. The dry portion of the ZTD can be accurately modelled with the observed surface pressure, while estimation of the wet portion of ZTD is a standard method in most post high-accuracy geodetic applications for the highly variability of the wet portion [15].

The tropospheric delay is then expressed as a linear combination of the dry and wet components [16];

$$D^{trop} = 10^{-6}\int_{path} N_d^{trop}\,ds + 10^{-6}\int_{path} N_w^{trop}\,da \tag{6}$$

or

$$D^{trop} = N_d^{trop} + N_w^{trop} \tag{7}$$

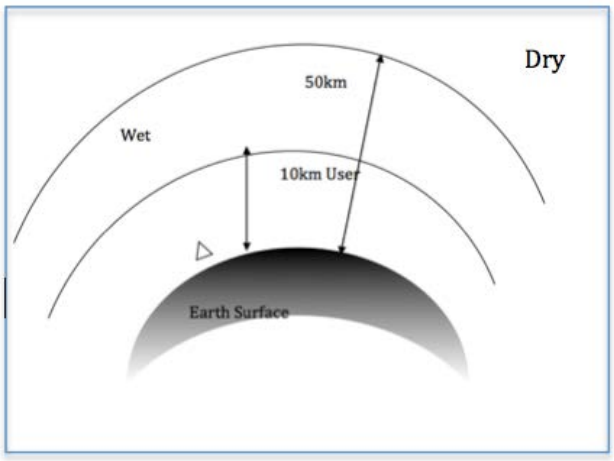

Figure 1. Thickness of polytropic layers for the troposphere. Modified after [13]

Tropospheric delay is calculated in the zenith direction over the GPS station, hence the term zenith tropospheric delay (ZTD), a combination of the zenith dry delay (ZDD) and zenith wet delay (ZWD). The tropospheric delay is a function of elevation and altitude of the receiver, which depends on factors such as atmospheric temperature, pressure and relative humidity. It is not frequency-dependent as is the case with the ionosphere and cannot be eliminated through linear combination of L1 and L2 observations [17].

3. Tropospheric Delay Models

Several global tropospheric models such as the Saastamoinen model, Hopfield model, Niell model etc. have been empirically developed and employed in GPS timing receivers to correct for the tropospheric delay. These models are derived using data from available

radiosonde obtained from Europe and North America continents. The global atmosphere conditions, used as constants in these models, provide a broad approximation of the tropospheric conditions, but ignore the actual atmospheric conditions on a given location, i.e., do not take into account the latitudinal and seasonal variations in the atmosphere [18]. Besides, daily variation in temperature, pressure and relative humidity can lead to error in tropospheric delays obtained using the global tropospheric models especially in the height components [19]. The location of Nigeria in the equatorial and tropical region makes it susceptible to high tropospheric effect thereby having an adverse effect on the GPS signals, which, in turn, affects positioning. In order to determine the best-fit tropospheric model for processing of data collected from the Nigerian Permanent GNSS Network, the need to investigate the impact of the different global tropospheric models on the network becomes imperative. The research investigates the performance of three global tropospheric delay models, namely Refined Saastamoinen model [20], Modified Hopfield model [3] and Niell model [21].

3.1. Davis et al Model

Davis et al expression slightly differs from the Saastamoinen model in the choice of the refractivity constant. [5] used the refractivity constant k1 given by [22]. Table 1 provides the refractivity constant K given by different authors. Davis et al model is given by the following expression [22]:

$$D_d^{trop} = \left[0.0022768 m/bar\right]\frac{P_s}{1-0.00266\cos 2\varphi - 0.0000028H} \quad (8)$$

where:
$\boldsymbol{P_s}$ = pressure at site
$\boldsymbol{\varphi}$ = geodetic latitude in radian
$\boldsymbol{H_s}$= surface height of station
K1 = 0.0022768.

3.2. The Refined Saastamoinen Model

The Saastamoinen model as in [20] is expressed as a function of height of the observation station and the zenith angle. This was later modified and functionally expressed as [23]:

$$D_z^{trop} = \frac{0.002277}{\cos z}\left[P + \left(\frac{1255}{T} + 0.05\right)P_w - B\tan^2 z\right] + \delta R \quad (9)$$

Where z = zenith angle of satellite
P = pressure (mbar)
T = temperature (K)
P_w = partial pressure of water vapour (mbar)
D_d^{trop} = tropospheric path delay in metres
B and δR are the corrections that depends on height (h) of the station and Z.

3.3. The Modified Hopfield Model

[13] used data from different parts of the world to develop an empirical tropospheric delay model. The Hopfield model shows dry and wet refractivity components as a function of tracking station height h above the Earth's surface and is given in the following forms [13]:

$$N_d^{trop} = N_{d,0}^{trop}\left[\frac{H_d - h}{H_d}\right]^{\mu} \quad (10)$$

$$N_w^{trop} = N_{w,0}^{trop}\left[\frac{H_w - h}{H_w}\right]^{\mu} \quad (11)$$

where $\mu = 4$ is empirically determined power of the height ratio, $H_d = 40136 + 148.72(T - 273.16)$ is the polytropic thickness for the dry part (m), $H_w = 11000$ is the polytropic thickness for the wet part (m), $N_{d,0}^{trop} = K_1\frac{P_0}{T_0}$ is the dry tropospheric refractivity for the stations at the Earth's surface as a function of pressure (millibars) and temperature (Kelvin), $N_{d,0}^{trop} = K_2\frac{e_0}{T_0} + K_3\frac{e_0}{T_0^2}$ is the wet tropospheric refractivity for the station at the Earth's surface as a function of water vapor, pressure, and temperature.

Inserting equations (9) and (10) into equation (6), and integrating each element with the respective integration ranges along the vertical direction (i.e. from h = 0 to h = H_d and from h = 0 to h = H_w for the dry and wet components), we then obtain tropospheric zenith delay in units of meters [16]:

$$T\frac{Z}{K} = \frac{10^{-6}}{5}\left[N_{d,o}^{trop}H_d + N_{w,0}^{trop}H_w\right]. \quad (12)$$

3.4. Black Model

[24] developed a tropospheric model based on Hopfield's work. [21] gives the formulas for the hydrostatic component as;

$$\delta S_{[HYD]} = \frac{1.552*10^{-5}\left[\frac{K}{hPa}\right].\frac{P_0}{T_0}.H_d}{\sqrt{1-\left(\frac{\cos\varepsilon}{1+I_c*\frac{H_d}{r}}\right)^2}} - \frac{1.92\left[\frac{m}{o}\right]}{\varepsilon^2 + 0.6^0}. \quad (13)$$

P_0: pressure at site in [hPa]
T_0: temperature at site in [K]
H_d: upper boundary height for the hydrostatic delay
r: radial distance from earth center to GPS antenna
ε: elevation angle in [degrees]

The wet mapping function derived by [24] is described by [25]. The slant-wet delay is express as [25]:

$$\delta S_{[WET]} = \frac{0.07465\left[\frac{K^2}{hPa}\right].\frac{e_0}{T^2}.H_T}{\sqrt{1-\left(\frac{\cos\varepsilon}{1+I_c*\frac{H_T}{r}}\right)^2}} - \frac{1.92\left[\frac{m}{o}\right]}{\varepsilon^2 + 0.6^0} \quad (14)$$

e_0: pressure at site in [hPa] and the mapping function is

$$m(\varepsilon)_{[WET]} = \frac{\delta S_{[WET]}}{\delta S_{[WET]}^{Z=0}} = \frac{\delta S_{[WET]}}{ZWD} = \frac{SWD}{ZWD}. \quad (15)$$

Table 1. Refractivity constant K1 according to different publications [26]

Reference	k_1 (khPa^{-1})	k_2 (khPa^{-1})	k_3 (khPa^{-1})	k'
[Boudouris, 1963]	77.59 ± 0.08	72.0 ± 11	3.75 ± 0.03	24 ± 11
[Smith and Weintraub, 1953]	77.61 ± 0.01	72.0 ± 0.09	3.75 ± 0.03	24 ± 9
[Thayer, 1974]	77.60 ± 0.01	64.79 ± 0.08	3.776 ± 0.004	17 ± 10
[Hill et al, 1982]	-	98 ± 1	3.583 ± 0.03	-
[Hill, 1988]	-	102 ± 1	3.578 ± 0.03	-
[Belvis et al, 1994]	77.60 ± 0.09	69.4 ± 2.2	3.701 ± 1.200	-

3.5. The Niell Model

The Niell Model is a combination of the Saastamoinen zenith path delay with Neil mapping functions [4]. The parameters (a, b, c) used in the dry and wet components of the models as expressed in equations (10) and (11) are calculated based on the interpolation of the average and seasonal variation (amplitude) values as functions of latitude and time given as [4]:

For the dry component:

$$m_{d(\varepsilon)} = \frac{1+\dfrac{a_d}{1+\dfrac{b_d}{1+c_d}}}{\sin\varepsilon + \dfrac{a_d}{\sin\varepsilon + \dfrac{b_d}{\sin\varepsilon + c_d}}} + \left[\frac{1}{\sin\varepsilon} - \frac{1+\dfrac{a_{ht}}{1+\dfrac{b_{ht}}{1+c_{ht}}}}{\sin\varepsilon + \dfrac{a_{ht}}{\sin\varepsilon + \dfrac{b_{ht}}{\sin\varepsilon + c_{ht}}}}\right] \cdot \frac{H}{1000}. \quad (16)$$

For the wet component:

$$m_{w(\varepsilon)} = \frac{1+\dfrac{a_w}{1+\dfrac{b_w}{1+c_w}}}{\sin\varepsilon + \dfrac{a_w}{\sin\varepsilon + \dfrac{b_w}{\sin\varepsilon + c_w}}} \quad (17)$$

where; m_d and m_w is the mapping functions for dry and wet components respectively; ε is the satellite elevation angle and H = orthometric height a_d, b_d, c_d are the coefficients in the dry component; a_w, b_w, c_w are the coefficients in the wet component and a_{ht}, b_{ht}, c_{ht} are the coefficients in the height component.

4. The Southern Nigerian GNSS Reference Network

The Office of the Surveyor General of the Federation (OSGoF) established the NIGerian Permanent GNSS NET work (NIGNET), which is a network of Continuously Operating Reference Stations (CORS). The goal is to implement a new reference frame for Nigeria in line with the recommendation of the United Nation Economic Commission of Africa (UNECA) through Committee on Development, Information Science and Technology (CODIST) [27]. It is expected that, the Nigerian Permanent GNSS Reference Network as presented in Figure 2, will directly contribute to the Africa Reference Frame (AFREF).

5. Materials and Methods

The use of network of reference stations, instead of the single reference station, has become widely acceptable within the GNSS community as solution for high precision satellite positioning applications [28]. This allows modelling of the atmospheric errors such as the tropospheric propagation delays that complicate the process of ambiguity fixing, which is often considered necessary for high-precision positioning and thus, significantly reducing the errors for long baselines thereby enhancing positioning accuracy.

5.1. Study Area

The study is in the Southern part of Nigeria as shown in Figure 3 which is made up of sixteen (16) states: Imo, Abia, Ekiti, Anambra, Enugu, Ebonyi, Osun, Ogun, Lagos, Oyo, Edo, Cross River, Rivers, Akwa-Ibom, Bayelsa, Delta and Ondo states. Observations were made on the GNSS campaign stations forming the Nigerian Primary Triangulation Network (NPTN). Figure 4 shows the ten (10) campaign stations forming the three networks (Network 1, 2 and 3) in the southern states of Nigeria. Table 2 shows the location of the stations across the study area.

5.2. Data Acquisition

The study area was divided into three networks. GPS campaigns were carried out on the network in the months of October 2010, March 2011 and April 2011; thus representing each campaign. Twenty-four hours (24hrs) raw GPS data at 30-second data rate were acquired. Corresponding precise satellite ephemeris were downloaded from the International GNSS Service (IGS) The ocean tide loading data for each station was obtained from [29]. Similarly, the Earth Orientation Parameters and the Ionosphere models were downloaded from [30]. Summary of the parameters used are given in Table 3.

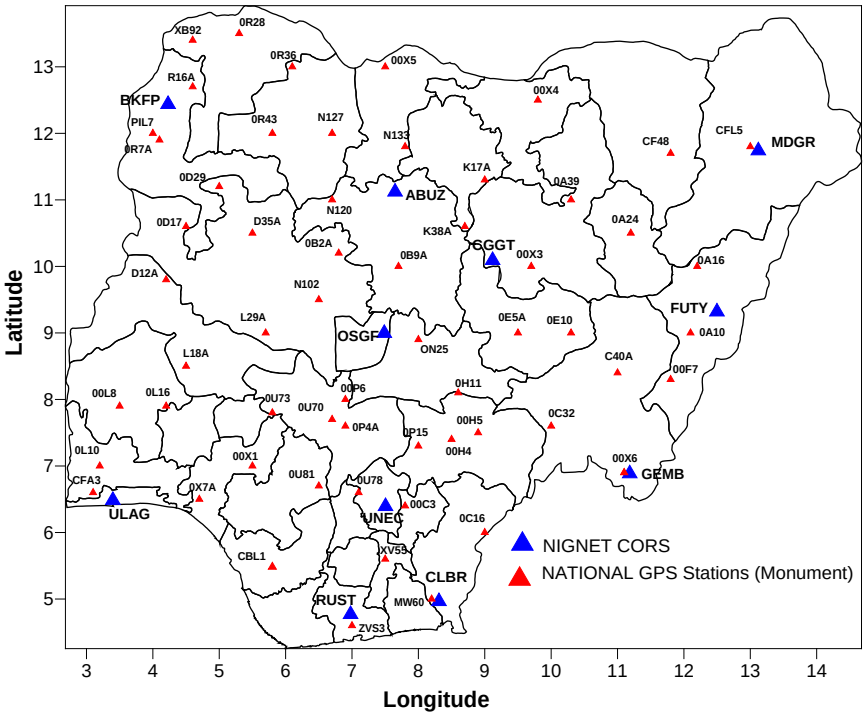

Figure 2. Nigerian CORS (blue) and Campaign (red) GNSS Stations (NIGNET) [31]

Figure 3. Map of the Campaign GNSS Triangulation Network in Southern States of Nigeri, [Authors]

Figure 4. The three (3) GNSS campaign networks used in this stuy [Authors]

Table 2. Description of the campaign GNSS Stations used in the Study

Station ID	Station locations	State	Approximate Lat.(N)	Approximate. Long.(E)	Ellipsoidal height (m)
OL10	Akomoge	Ogun	7° 12' 15.839"	3° 20' 41.494"	198.953
OL16	Oke Onwa	Oyo	7° 54' 14.814"	4° 24' 13.707"	524.882
CFA3	Ikeja	Lagos	6° 37' 36.856"	3° 19' 23.231'	71.871
OX7A	Okitipupa	Ondo	6° 30' 02.670"	4° 46' 30.570"	59.585
ZVS3	Port Harcourt	Rivers	4° 50' 52.690"	7° 02' 52. 52.8"	35.4829
CBL1	Shell Camp	Delta	5° 33' 16.660"	5° 43' 56.38"	26.480
OU81	Ugboha	Edo	6° 47' 13.241'	6° 29' 08.215"	215.814
OC16	Abu Emeh	Cross Rivers	6° 08' 13.427"	9° 01' 35.849'	628.828
MW60	Odukpani	Cross Rivers	5° 07' 19.312'	8° 20' 19.783'	105.464
XV55	Okpotong	Abia	5^0 33' 21.801'	7° 38' 18.397"	154.966

Table 3. Summary of General Processing Parameters

Parameter	Description
RINEX data	30 second sampling rate
Orbital Data	IGS final/Pricise orbit
Processing window	24 hours sliding window
Ocean tide loading	FES 2004
Reference Frame	ITRF 2008
Satellite Elevation Angle	10^0 Cut-off
Double Difference Ionosphere	Quasi-Ionosphere free (L_3) ambiguity free
Mapping Function	Troposphere delay mapping function of $^1/_{cosz}$
Adjustment	All Stations coordinate minimally constrained to their apriori

5.3. Processing Strategy

Six (6) processing strategies were employed using the Trimble Total Control (TTC) version 2.73. They include:

Strategy I: In this strategy, the processing is done without the application of the tropospheric model. The ionosphere-free double difference (IF DD) residuals and final coordinates are extracted for analysis.

Strategy II: Processing with the application of the Black model and standard atmosphere, the IF DD residuals, final coordinates and the zenith tropospheric delay are extracted for analysis.

Strategy III: Processing with the application of the Davis et al model and standard atmosphere; the IF DD residuals, final coordinates and the zenith tropospheric delay are extracted for analysis.

Strategy IV: Processing with the application of the Hopfield model and standard atmosphere; the IF DD residuals and final coordinates are extracted for analysis purpose.

Strategy V: Processing with the application of the Neil model and standard atmosphere; the IF DD residuals and final coordinates are extracted for analysis purpose.

Strategy IV: Processing with the application of the Saastamoinen model and standard atmosphere; the IF DD residuals and final coordinates are extracted for analysis purpose.

The coordinates of all stations were estimated. This retains the flexibility for later changes in the realization of the reference frame. However, to check the consistency of the data used in the processing with the coordinates of the IGS core sites, a minimal constraint solution was generated for the network.

6. Results and Discussions

The analysis of the results was done based on the Ionospheric Free Double Difference (IF DD) residuals in the baseline domain, the final station coordinates and the zenith tropospheric delay obtained from each of the global tropospheric delay model, in order to ascertain the best fit tropospheric delay model for the study area.

6.1. Assessment of the Tropospheric Delay Models on the Basis of the Baseline Ionospheric-free Double Difference (IF DD) Residual

One of the tools used in the assessment of tropospheric model in a GPS network is the comparison of the baseline IF DD residuals over which the tropospheric models are being assessed [16]. The Root Mean Square Error (RMSE) characterizes the performance of the models. The IF DD of each of the 3 networks was analysed. Baselines were formed and the RMSE were computed for all satellites.

Table 3 to Table 5 summarises the numerical results for all the baselines in terms of the RMS IF DD residuals in the three networks. The IF DD residuals of strategy I (No model) have large residuals compare to strategies II, III, IV and V respectively. This is expected because no model is applied. The result indicates that, the five models are able to reduce the size of the residuals. However, no significant residual difference in the five models is noticed in the three networks. In Table 4 - Table 6, the long baselines, OC16-ZVS3; OU81-ZVS3 and CFA3-OL16 have the highest rmse values across the models in the

three networks; while the short baselines, XV55-ZVS3; ZVS-XV55 and CFA3-OL10 have the shortest rmse values. This indicates that, the longer the baseline, the more the effects of the troposphere. This presupposes that, the tropospheric delay is a distance-dependent error. This result is in agreement with [32]. The Neil model gives a better result with less effects of the troposphere on the baselines across the three networks in the study area.

Figure 5 – Figure 7 provides the percentile improvement in the RMS DD IF residuals for strategies II, III and IV and V respectively. From the figures, the result shows that baseline percentage improvement varies from 67% to 71% in network, 62% to 76% in network 2 and 71% to 76% in network 3. The Niell model receives the least percentage improvement contribution in the network with an average of 67.1%. Davis et al, the modified Hopfield and Saastaminen models have 70%, 71.1% and 71.7% respectively. This suggests that, the Neill model reduces the effect of the delay cause by the troposphere more than the other the rest of the models assessed in this work.

Table 4. Network 1 summary statistics of baseline RMS DD IF residual

Baseline	Baseline Length (km)	Total RMS (mm) of IF DD					
		No Model	Black Model	Davis et al Model	Hopfield Model	Saastamoinen Model	Niell Model
0C16-ZVS3	261.552	30.7	21.0	21.0	21.0	21.0	20.0
MW60-0C16	135.676	29.5	17.9	17.8	18.4	19.9	18.2
XV55-0C16	166.632	24.6	22.1	16.3	17.1	16.3	16.0
XV55-MW60	91.271	19.7	15.0	15.0	15.1	15.1	14.8
XV55-ZVS3	102.073	21.7	14.0	14.0	14.2	14.0	13.9
ZVS3-MW60	146.348	20.4	13.7	13.7	13.7	15.8	13.4

Table 5. Network 2 summary statistics of baseline RMS DD IF residual

Baseline	Baseline Length (km)	Total RMS (mm) of IF DD					
		No Model	Black Model	Davis et al Model	Hopfield Model	Saastamoinen Model	Niell Model
0U81-CBL1	161.345	35.1	25.1	25.1	25.2	24.9	25.2
0U81-XV55	186.575	29.9	19.0	19.0	18.9	19.0	18.9
XV55-CBL1	211.212	20.3	16.9	16.9	16.9	16.9	16.9
0U81-ZVS3	223.288	18.8	26.2	25.3	25.3	25.6	24.8
ZVS3-CBL1	164.595	31.2	20.8	20.8	20.8	20.7	20.8
ZVS3-XV55	102.073	18.5	11.0	11.0	11.0	11.0	11.0

Table 6. Network 3 summary statistics of baseline RMS DD IF residual

Baseline	Baseline Length (km)	Total RMS (mm) of IF DD					
		No Model	Black Model	Davis et al Model	Hopfield Model	Saastamoinen Model	Niell Model
CFA3-0X7A	161.195	18.6	14.8	14.8	14.8	14.8	12.8
0X7A-OL10	176.205	17.9	14.8	14.8	14.8	14.8	13.8
CFA3-OL10	63.912	17.3	12.7	12.7	12.7	12.7	12.3
0X7A-OL16	160.535	18.5	14.2	14.1	14.2	14.1	13.2
CFA3-OL16	184.925	24.1	18.6	18.5	18.6	18.5	18.3
OL16-OL10	140.170	19.1	15.4	14.4	15.4	14.4	13.6

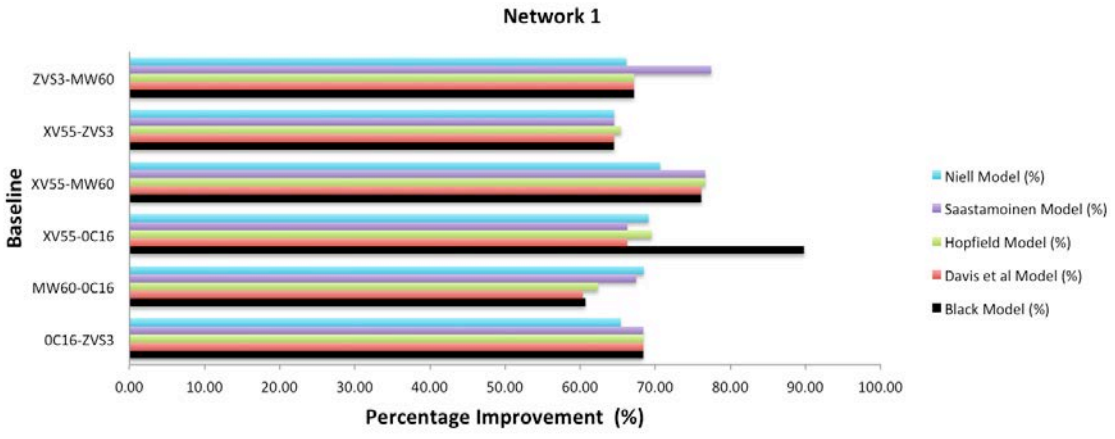

Figure 5. Network 1 percentage improvement DD IF residuals after applying tropospheric delay models

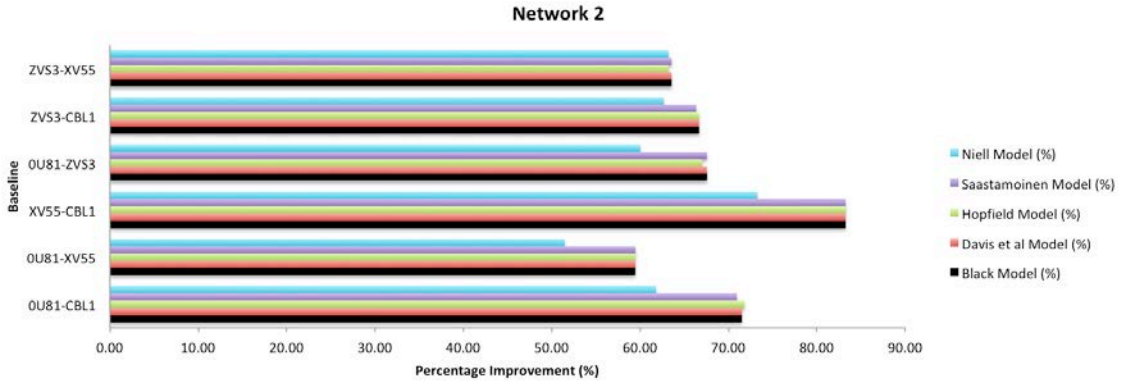

Figure 6. Network 2 percentage improvement DD IF residuals after applying tropospheric delay models

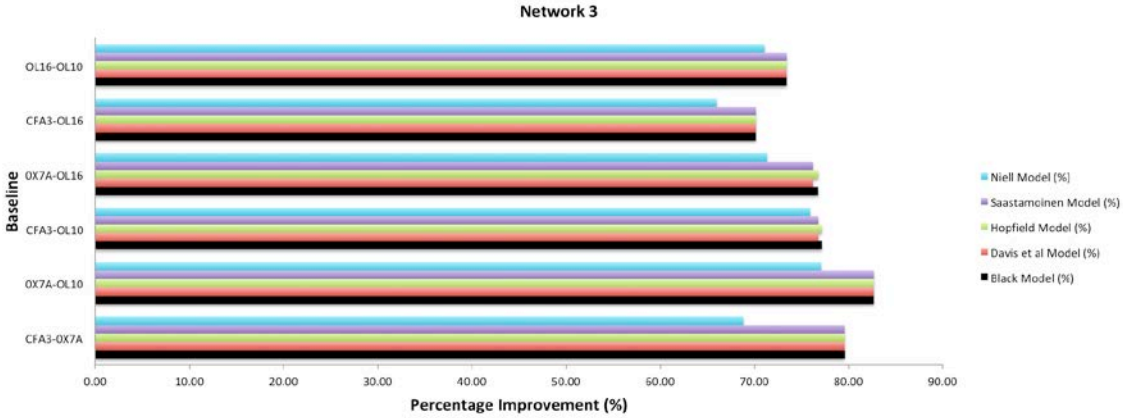

Figure 7. Network 3 percentage improvement DD IF residuals after applying tropospheric delay models

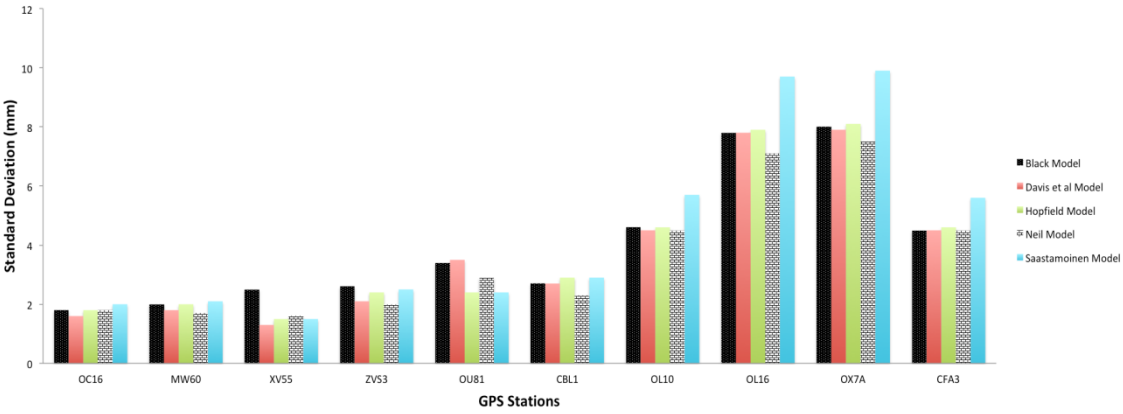

Figure 8. Mean standard deviation in the North component

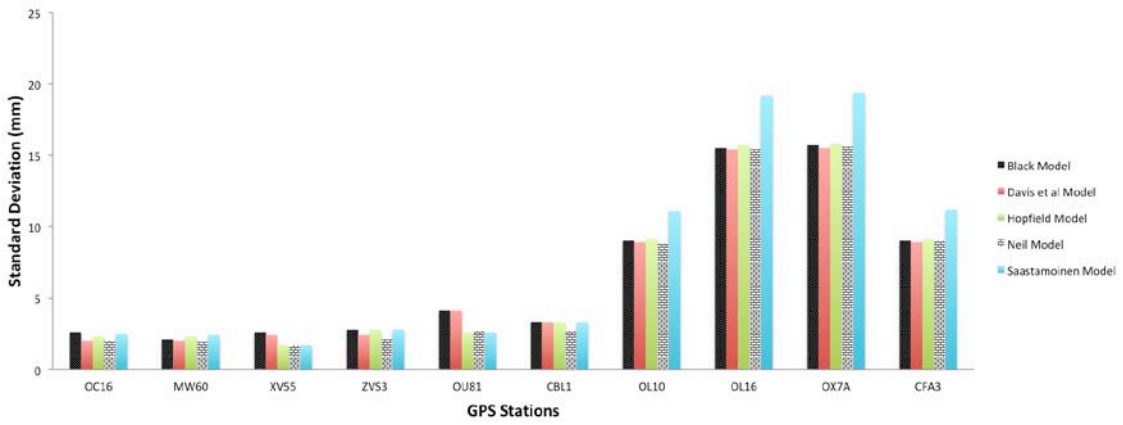

Figure 9. Mean standard deviation in the East component

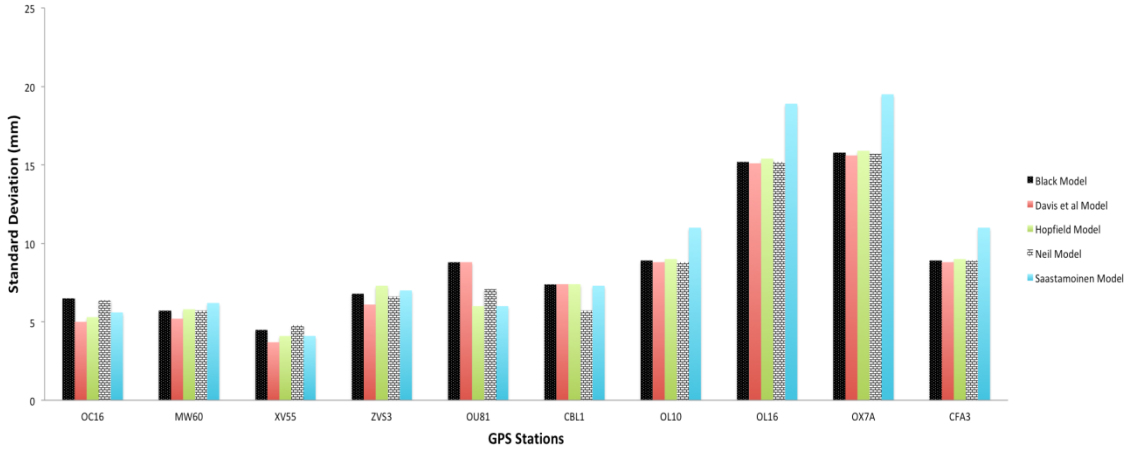

Figure 10. Mean standard deviation in the Height component

6.2. Assessment of the Tropospheric Models in the Position Domain

To study the tropospheric delay models in the position domain, the coordinate differences of the stations in the North, East and Height (horizontal and height) components were computed and analysed. Figure 8, Figure 9, and Figure 10 shows the mean standard deviation of the coordinates in North, East and Height components at the GNSS stations.

The result reveals that, the Niell and Hopfield models show no significant deviations in the North and East components respectively.

However, the differences in the application of the tropospheric delay models reveals that, the Niell model shows considerable improvement with network average standard deviation of 3.5mm, 6.0mm and 8.4 in the north, east and height component respectively, while the Davis et al Model followed closely with network average standard deviation of 3.7mm, 6.5mm and 8.5mm in the north, east and height components respectively.

6.3. Mean Zenith Tropospheric Delay (ZTD) at Each Station

The tropospheric delay is calculated in the zenith direction over the GNSS station. The Zenith Tropospheric Delay (ZTD) gives insight into the tropospheric conditions above the GPS site. Table 7 show the statistics of the zenith tropospheric delay for each of the GNSS station based on the application of each tropospheric delay model. The mean ZTD computed at each station reveals that, station ZVS3 latitude 4^0 $50^{'}$ 52.69" has the highest average ZTD value of about 2.645m. This is followed by station MW60 at latitude 5^0 07' 19.31" having average ZTD value of about 2.626m. However, station OL16 located at the highest latitude of about 07^0 54' 14.814" in the entire network have the least ZTD value of about 2.440m. This result presupposes that, GNSS stations at low latitude are highly susceptible to tropospheric delay. This can be seen in Figure 11 showing the spatial distribution of the tropospheric delay in Southern Nigeria. The figure reveals that, GNSS stations in Southern Nigeria particularly in Rivers, Bayelsa, Lagos, Cross River and Delta states are highly susceptible to the effect of the troposphere when compare to other states in Southern Nigeria. This result is in agreement with [32] who assert that, GNSS stations at low latitude are highly susceptible to tropospheric effect.

The mean network ZTD produced by the five tropospheric delay shows that the Niell model has the lowest network ZTD of 2.535m with mean RMS value of 0.67m, follow by Davis et al model with network ZTD of 2.559m and mean RMS value of 0.72m. The Black model has the highest mean network ZTD of 2.588m with mean RMS value of 0.78m.

Table 7. Statistics of the mean network ZTD estimate at each GNSS station

GPS Station	Zenith Tropospheric Delay Models (m)				
	Black Model	Davis et al Model	Hopfield Model	Neil Model	Saastamoinen Model
OC16	2.5269	2.4258	2.5251	2.4240	2.4231
MW60	2.6207	2.6203	2.6202	2.5801	2.6199
XV55	2.5929	2.5926	2.5916	2.5904	2.5889
ZVS3	2.6422	2.6417	2.6415	2.6012	2.6409
OU81	2.5149	2.5049	2.5148	2.5046	2.5141
CBL1	2.6077	2.6084	2.6089	2.5793	2.6098
OL10	2.5425	2.5425	2.5426	2.5209	2.5430
OL16	2.5976	2.4177	2.5176	2.4071	2.4163
OX7A	2.6047	2.6050	2.6057	2.5764	2.6068
CFA3	2.6288	2.6289	2.6292	2.5694	2.6297
Mean Network ZTD	**2.5879**	**2.5588**	**2.5797**	**2.5353**	**2.5593**

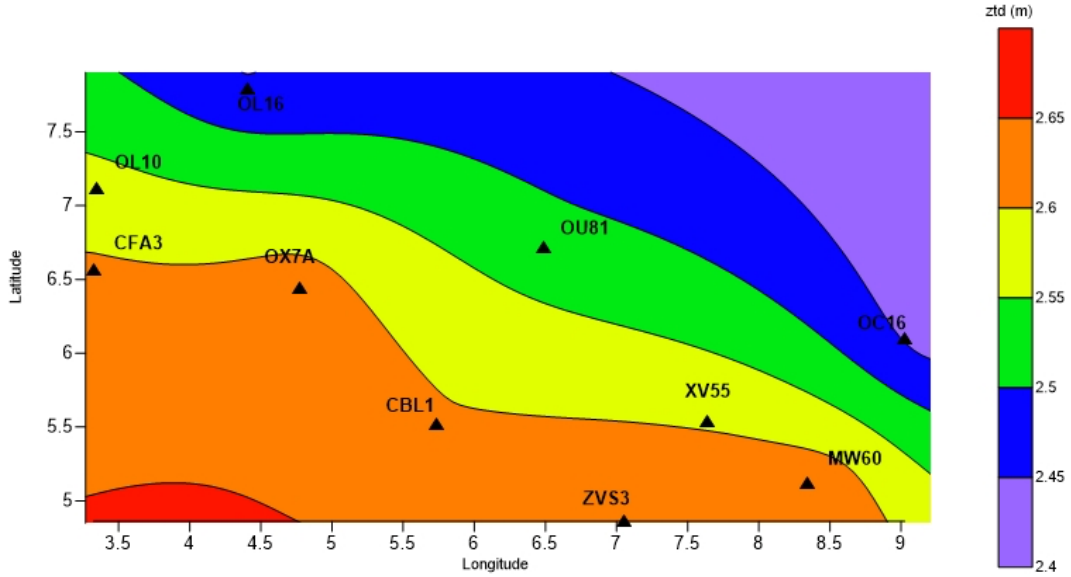

Figure 11. Spatial Distribnution of the Total Zenith Tropospheric Delay of the study area

7. Conclusion

A total of eighteen baselines, thus making the three networks were analyzed. The study shows that the troposphere delay affect long baselines the more than short baselines, this agrees with [12] and [32]. This validates the assertion that, tropospheric delay is a distance dependent error.

The five models investigated i.e. the Black, Davis et al, Hopfield, Neill and Saastamoinen models show no significance difference in their performance; better improvements in the position domain were achieved by the application of the Niell model compared to the rest of the models. The Niell model produced a better mitigation of the tropospheric delay, with an average percentage improvement of 67.1%; while Davis et al, the modified Hopfield and Saastaminen models have 70%, 71.1% and 71.7% percentage improvement respectively. The result also indicates that, the Niell has the lowest mean average zenith tropospheric delay (ZTD) of 2.535m with RMS of 0.67m. On the overall, the Niell model has better performance in the network in this research. This result is in agreement with [33].

Acknowledgements

The authors acknowledge the Office of the Surveyor General of Nigeria for providing the data used in this research.

References

[1] Russel, R. (2010). The toposphere, Window to the Universe. Retrieved from http://wwww.windows2universe.org.Last accessed January 10, 2017.

[2] Saastamoinen, J, "Atmospheric Correction for Troposphere and Stratosphere in Radio Ranging of Satellites", *Geophysical Monograph*, American Geophysical Union, Washington D.C. 247-252. 1972.

[3] Hopfield, H. S, "Two Quartic Tropospheric Refractivity Profile for Correcting Satellite Data". *Journal of Geophysical Research* 74(18), 4487-4499. 1969.

[4] Niell, A.E, "Global Mapping for the Atmospheric Delay at Radio Wavelenghts", *Journal of Geophysical Research* 111 (B2), 3227-3246. 1996.

[5] Davis, J. L., Herring, T. A., Shapiro, I. I., Rogers, A. E. E., & Elgered, G. "Geodesy by radio interferometry: Effects of atmospheric modelling on estimates of baseline length. *Radio Science*, 20(6), 1593-1607. 1985.

[6] Opaluwa, Y. D., Adejare, Q. A., Suleyman, Z. A. T., Abazu, I. C., Adewale, T. O., Odesanmi, A. O., & Okorocha, V. C. "Comparative analysis of five standard dry tropospheric delay models for estimation of dry tropospheric delay in GNSS positioning". *American Journal of Geographic Information System*. *2*(4), 121-131. 2013.

[7] Jorge, M. A., Lawrence, L., Yu-Ting, T., and Terry, M. "Analysing the Zenith Tropospheric Delay Estimates in On-line Precise Point Positioning (PPP) Services and PPP Software Packages" *Sensors (Basel)*. 18(2): 580. 2018.

[8] Sobhy, A., Y. "Modeling investigation of wet tropospheric delay error and precipitable water vapor content in Egypt" *The Egyptian Journal of Remote Sensing and Space Sciences* 19, 333-342. 2016.

[9] Mendes, V.B., and Langley, R.B., "Tropospheric zenith delay prediction accuracy for airborne GPS high-precision positioning. In: *Proceedings of The Institute of Navigation 54th Annual Meeting*, pp. 337-347, Denver, CO, U.S.A., 1-3 June. 1998.

[10] Bevis, M., Businger, S., Herring, T.A., Rocken, C., Anthes, R.A., Ware, R.H., "GPS meteorology: sensing of atmospheric water vapor using the global positioning system" J. Geophys. Res. 97 (D14), 15787-15801. 1992.

[11] Businger, S., Chiswell, S.R., Bevis, M., Duan, J., Anthes, R.A., Rocken, C., Ware, R.H., Exner, M., Solheim, F.S., "The promise of GPS in atmospheric monitoring". *Bull. Am. Meteorol. Soc*. 77 (1), 5-18. 1996.

[12] Dodo, J. D., Ojigi, L. M., & Tsebeje, S. Y. "Determination of the best-fit tropospheric delay model on the Nigerian permanent GNSS network". *Journal of Geosciences and Geomatics*, *3*(4), 88-95. 2015.

[13] Hofmann-Wellenhof, B., Lichtenegger, H. and Collins, J, *GPS, Theory and Practice*, Springer-Verlag Wien, New York. 2001

[14] Ahn, Y. W., Lachapelle, G., Skone, S. and Sahm, S. "Analysis of GPS RTK Performance using External NOAA Tropospheric Corrections Integrated with a Multiple Reference Station Approach", *GPS Solution*, 10, 171-186. 2006.

[15] Hongxing Z., Yunbin, Y., Wei L., Ying L., and Yanju C. "Assessment of Three Tropospheric Delay Models (IGGtrop, EGNOS and UNB3m) Based on Precise Point Positioning in the Chinese Region". *Sensors (Basel)* 16(1), 122. 2016.

[16] Don, K., Sunil, B., Langley, R. B., Dare, P. "Performance of Long-Baseline real-Time Kinematic Applications by Improving Tropospheric Delay Modelling", *ION GNSS International Technical Meeting of the satellite Division.* Long Beach, California, USA. 2004.

[17] Satirapod, C., and Chalermwattanachai, P, "Impact of Different Tropospheric Models on GPS Baseline Accuracy: Case Study in Thailand", *Journal of Global Positioning Systems*, 4(1-2), 36-40. 2005.

[18] Roberts, C., and Rizos, C, "Mitigating Differential Troposphere for GPS-based Valcano Monitoring", *5th International Symposium on Satellite Navigation Technology and Applications.* Canberra, Australia. 2001.

[19] Dodo, J. D., and Kamarudin, M. N. "Investigation on the Impact of Tropospheric Models on baseline precision in a local GPS network: Case of the Malaysian RTKnet", *Journal of Geomatics.* 2 (1), 137-142. 2008.

[20] Saastamoinen, J, "Contribution to the theory of Atmosphere Refraction", *Bulletin of Geodesique* (105, 106, 107): 279-298, 383-397, 13-34. 1973.

[21] Leick, A, *GPS Satellite Surveying,* USA: John Willey & Sons, Inc, 2004.

[22] Thayer, G. D. "An improved equation for the radio refractive index of air". *Radio Science*, *9*(10), 803-807. 1974.

[23] Guochang, X, *GPS Theory, Algorithms and Application*, Springer-Verlag Berlin Heidelberg, New York. 2003.

[24] Black, TH. L. "The New NMC Mesoscale Eta Model: Description and Forecast Examples" *Weather and Forecasting*, Vol. 9, pp. 265-278, June 1994.

[25] Seeber, G. *Satellite Geodesy*. Walter GeGruyter 2003.

[26] Mendes, V.B. "Modeling the neutral-atmosphere propagation delay in radiometric space techniques". *Doctor of Philosophy*, University of New Brunswick, Fredericton, Canada. 1999.

[27] Jatau, B., Fernandes, R.M.S., Adebomehin, A., and Goncalves, N "NIGNET-The New Permanent GNSS Network of Nigeria", *FIG Congress 2010 Facing the Challenges – Building the Capacity Sydney*, Australia, 11-16 April 2010.

[28] Vollath, U., Buecherl, A., Landau, H., Pagels, C. and Wagner, B, "Multi-Base RTK Positioning Using Virtual Reference Stations",*Institute of Navigation, ION GPS-2000*, Salt Lake City, 22-19 September, 123-131.2000.

[29] "Ocean Tide Loading" Available: http://www.oso.cha. [AccessedSept. 20, 2009].

[30] "The Earth Orientation Parameters and the Ionosphere models" Available: http://www.bernese.unnibe.ch/ [Accessed: Sept. 21, 2009].

[31] Dodo, J. D. "The Geocentric Datum of Nigeria (GDN2012)". *A Technical Report*, Office of the Surveyor General of Nigeria. Abuja. 2012.

[32] Tajul, A. M., Lim, S., Yan, T. and Rizos, C. "Mitigation of Distance-Dependent Errors for GPS Network Positioning". *International Global Navigation Satellite Systems Society IGNSS Symposium*, Surfers Paradise, Australia. 2006.

[33] Péter, B. "The evaluation of troposphere models applied in the Hungarian Active GNSS Network" *The Council of European Geodetic Surveyors* 2012.